



Development of a numerical model for sediment yield for the upper Brahmaputra River basin using optimization technique

Briti Sundar Sil¹ · Shehnaj Ahmed Pathan¹

Received: 6 September 2022 / Accepted: 12 December 2022 / Published online: 29 December 2022

© The Author(s) under exclusive licence to Institute of Geophysics, Polish Academy of Sciences & Polish Academy of Sciences 2022

Abstract

At a watershed scale, soil erosion occurs at a spatially variable rate, posing a significant danger to long-term resource management. The most serious issue has long been regarded as soil erosion. As a result, estimating soil loss and identifying the critical area for implementing optimum management techniques are essential to the programme's success. A numerical model called the sediment-rainfall-watershed area model (SRWA) is built using a spatially distributed RUSLE-based SDR hybridized model to estimate sediment yields in the upper Brahmaputra River watershed. The developed model has been calibrated and validated from 2001 to 2007 and 2008 to 2014, respectively. For the entire period, the statistical performance of the proposed SRWA model and the SDR-RUSLE-based model reveals a correlation coefficient of 0.93 and a Nash–Sutcliffe efficiency coefficient of 0.84. This demonstrates that the SRWA model may assess sediment yield at any upper Brahmaputra basin watershed/sub-watershed outlet.

Keywords GRG nonlinear · Sediment yield · Majuli river island · Brahmaputra River basin · RUSLE · GRG nonlinear

Introduction

Soil degradation is currently the most severe environmental problem worldwide, as it depletes topsoil nutrients, degrades agricultural land, and diminishes crop output (Pradeep et al. 2015). In a watershed, soil erosion can lead to severe land degradation issues. Recently, it has been found that researchers are actively working on analysing soil erosion and sediment yield, mainly focusing on tropical and subtropical regions (Issaka and Ashraf 2017). Globally, the annual soil erosion rate from cultivated land ranges from 22 to 100 tonnes per hectare (Girmay et al. 2020). One-third of the world's agricultural area is believed to be affected by soil erosion (Hurni and Meyer 2002). According to estimates from an assessment of soil deterioration in India, water and wind erosion affected around 1100 million hectares and 550 million hectares, respectively (Saha 2003). In the Himalayas and

the Western Ghats, soil erosion affects about 45 per cent of the land area. Soil disintegration directly impacts the massive production of sediments and rapid deposition in watersheds. Human-caused soil deterioration affects approximately 1964.4 million hectares (M ha) of soil globally, with water erosion exacerbating the problem in 1903 M ha (Bhattacharyya et al. 2015). Several experts identified soil loss as a serious threat in mountainous areas. In the Brahmaputra basin highlands, this situation is particularly acute. An accurate estimation of soil erosion amount is required to determine the effect of soil erosion on a regional scale. A massive amount of silt in runoff water causes sedimentation of river beds and flood disasters; as a result, effective control and supervision should be a critical component of watershed planning and management (Xu et al. 2015). Because of its adaptability under a variety of ecosystem types and management scenarios, the RUSLE model is used in several studies to estimate net and average soil loss and sediment discharge at river outlets for various watersheds (Jain and Kothiyari 2000; Ganasri and Ramesh 2016; Alewell et al. 2019; Li et al. 2020; Yadav et al. 2022). Manual or mechanical methods of assessing the above components with adequate precision for calculating soil loss are time-consuming and uneconomical because of the delicate interaction between climate, LULC, and other anthropogenic activities involved in a watershed (Duru et al.

Edited by Dr. Robert Bialik (ASSOCIATE EDITOR) / Dr. Michael Nones (CO-EDITOR-IN-CHIEF).

✉ Shehnaj Ahmed Pathan
shehnajpathan9@gmail.com

¹ Department of Civil Engineering, National Institute of Technology, Silchar 788010, India

2018). Many empirical models based on geomorphological factors were constructed to calculate previous soil loss and quantify sediments output. Several approaches are widely used, including the sediment yield index (SYI), the Universal Soil Loss Equation (USLE), and the Revised Universal Soil Loss Equation (RUSLE) (Renard 1997; Wischmeier and Smith 1978). As the USLE model and its revised form (RUSLE) can only measure soil loss and do not account for sediment transportation or deposition, the sediment delivery ratio (SDR) model is frequently used in conjunction with the USLE or RUSLE to assess the soil loss and sediment yields at the same time (Jain and Kothiyari 2000). Using traditional approaches like a hydrographic survey to estimate sediment deposition in a watershed is time-consuming. It takes a lot of time and human resources, and it is not even cost-effective. Many researchers have used the RUSLE-SDR model to evaluate soil erosion and sediment production in various sites due to its high efficiency and ease of application (Gelagay 2016; Poirier et al. 2016; Yan et al. 2018). However, reliable measurement and erosion prediction become challenging because of the number of very sensitive and complex variables in the process of soil erosion. The ability to assess sediment yield has ramifications since it could be a useful tool in guiding future river management efforts. Advanced data-driven technologies, such as machine learning approaches and the generalized reduced gradient (GRG) nonlinear method, have been demonstrated to be effective in modeling environmental and natural resource modeling (Wenzel Jr and Melching 1987; Mirzaei et al. 2018; Hosseini et al. 2020; Niazkar and Zakwan 2021). For sediment rating curves and sediment yield in a watershed, the GRG nonlinear technique appears to outperform standard models (Vale et al. 2016; Zakwan and Ahmad 2021; Jabbar and Yadav 2022).

The Brahmaputra River watershed is one of the largest watersheds and carries massive sediment. The largest river island, Majuli, is formed because of the sediment deposition over the decades. As mentioned, the Brahmaputra basin yields a large amount of sediment every year. The formation of sand bars occurs throughout its course, and the river has become a braided river. Therefore, an assessment of the sediment yield at the outlet of each sub-watershed will provide a clear view of the sediment transport scenario. In the literature, it is found that spatially distributed models like the RUSLE-SDR model can be used accurately to assess soil loss as well as sediment yield from a watershed. Similar to other erosion models, RUSLE-SDR is a multi-input model. Still, some of its input parameters may not have all spatial data at the watershed scale for sediment yield estimation. And also, some inputs may not have good quality satellite images, requiring high computational techniques. Therefore, the output may not necessarily have satisfactory results. Moreover, obtaining reliable results from the RUSLE-SDR model depends on skilled professional opinions regarding

data selection and methods for the computation of model inputs. Therefore, a numerical model that provides a simple technique and ease for estimation may help the engineers and planners quickly assess the same. Considering this aspect, it is intended to develop a numerical model based on the RUSLE-SDR model in this study. So, to develop the model, the sediment yields at different watershed levels are estimated considering outlets at various locations in the same river using the RUSLE-SDR model. After generating the data for sediment yield for about 14 years, a numerical model is developed using GRG nonlinear optimization technique with satisfactory performance statistics. The detailed study area, the methodology adopted, and the step-by-step procedure are discussed further in the following texts.

Study area and input data

Study area

The current study focuses on the Upper Brahmaputra River Basin (UBRB) up to Majuli River Island. It lies between longitude 84° 30' E to 95° 30' E and latitude 25° 00' N to 31° 30' N, as shown in Fig. 1. The study area covers a total area of about 372,385 km². It is located at an elevation between 10 and 7312 m above mean sea level (Fig. 3a). Seasonal flow, silt transport, and channel structure are the essential characteristics of the Brahmaputra River (Mani et al. 2003). Due to frequent inundation and eroded floodplains damaging land and crops in the Brahmaputra valley and north bank tributaries, the Upper Brahmaputra valley is the worst flood-affected area (Hazarika et al. 2015). The tremendous inundation of the river Brahmaputra every year significantly impacts Majuli. The river flows in a firmly braided channel with multiple laterals, mid-channel bars, and islands in the Brahmaputra valley. The majority of them are transient, drowned during large rainy season flows, significantly varying geometry and locations. Majuli, the world's largest river island, is facing extinction due to the river's severe erosion problem (Mani et al. 2003). The Brahmaputra River has an average discharge of 20,000 m³/s. The basin's climate is monsoon-driven, with a distinct rainy season that lasts from June to October and accounts for 60–70% of yearly precipitation (Immerzeel 2008). Immerzeel (2008) classified the Brahmaputra watershed into three physiographic zones: the Tibetan Plateau (TP), the Himalayan Belt (HB), and the Floodplain (FP). The Upper Brahmaputra basin, which includes China, Bhutan, and India, consists of TP and HB.

Input data

The dataset essential for evaluating RUSLE factors and generating erosion hazard maps is prepared from

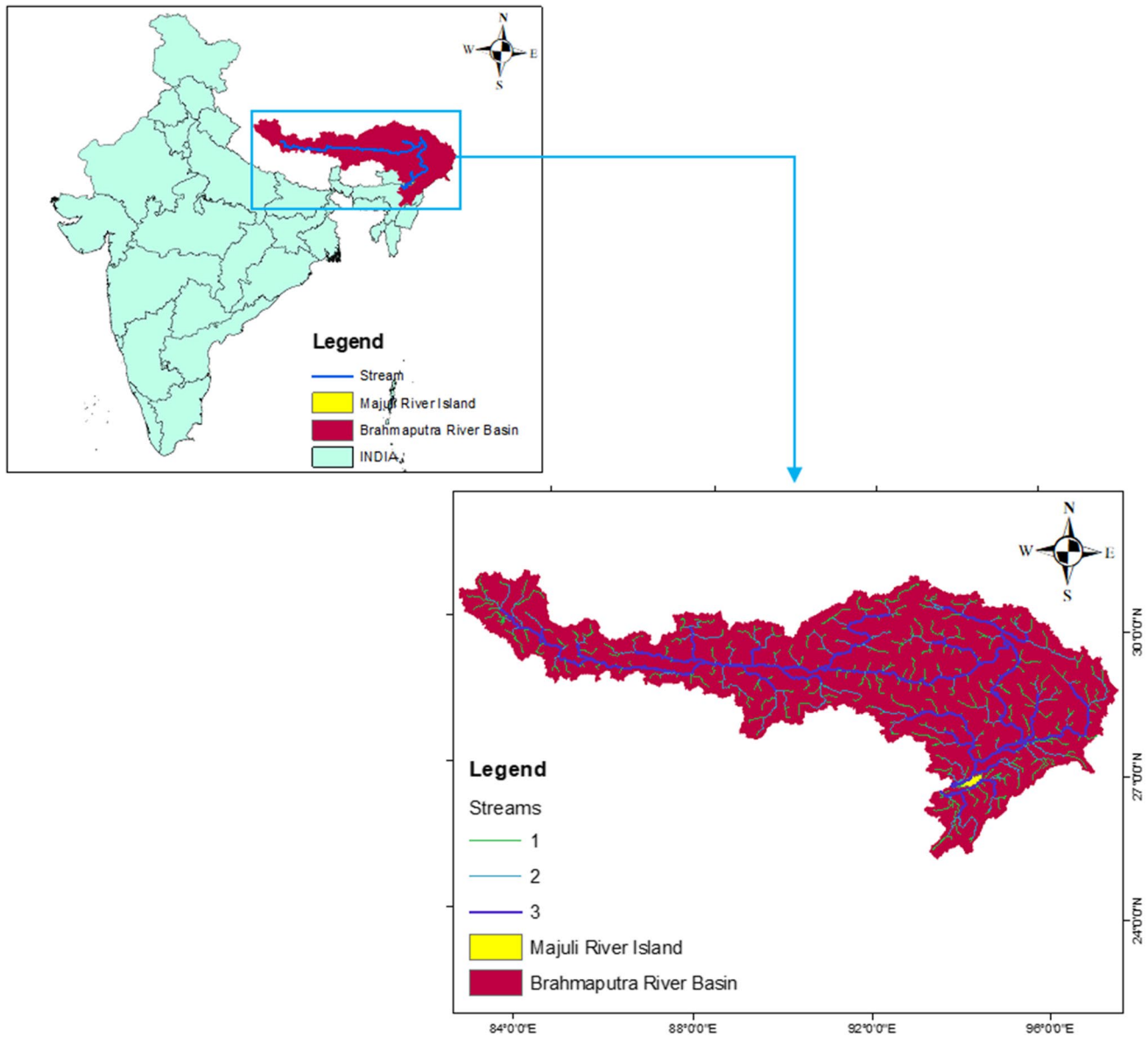


Fig. 1 Study Area map showing Brahmaputra River watershed up to Majuli River Island

various data sources. The digital elevation model (DEM) is obtained from <https://lpdaac.usgs.gov/>. The DEM is in 1 Arc Second (30 m) resolution (Fig. 2a). A soil map is downloaded from FAO DSMW (Fig. 2b). It is on a 1:5,000,000 scale and is classified into eleven categories following the UNESCO-FAO soil classification scheme (Table 1). The land use/land cover (LULC) maps for 2001–14 are MODIS land cover type (MCD12Q1). This product is downloaded from USGS earth explorer. Then, it is imported into Arc GIS and is classified into eight new LULC classes (Fig. 2c). It can be seen that forests and grasslands have occupied most parts of the watershed (Table 2). In some parts of the Himalayan region, all rainfall data are not available. Therefore, precipitation data

are obtained from Climate Forecast System Reanalysis (CFSR). Daily rainfall data from 2001 to 2014 for 357 stations are prepared for the basin (Fig. 2d).

Methodology

In this context, we have discussed the distributed model RUSLE and SDR through which we have calculated the sediments amount at the outlet of each watershed. We have also discussed the newly developed SRWA model and the GRG nonlinear optimization technique.

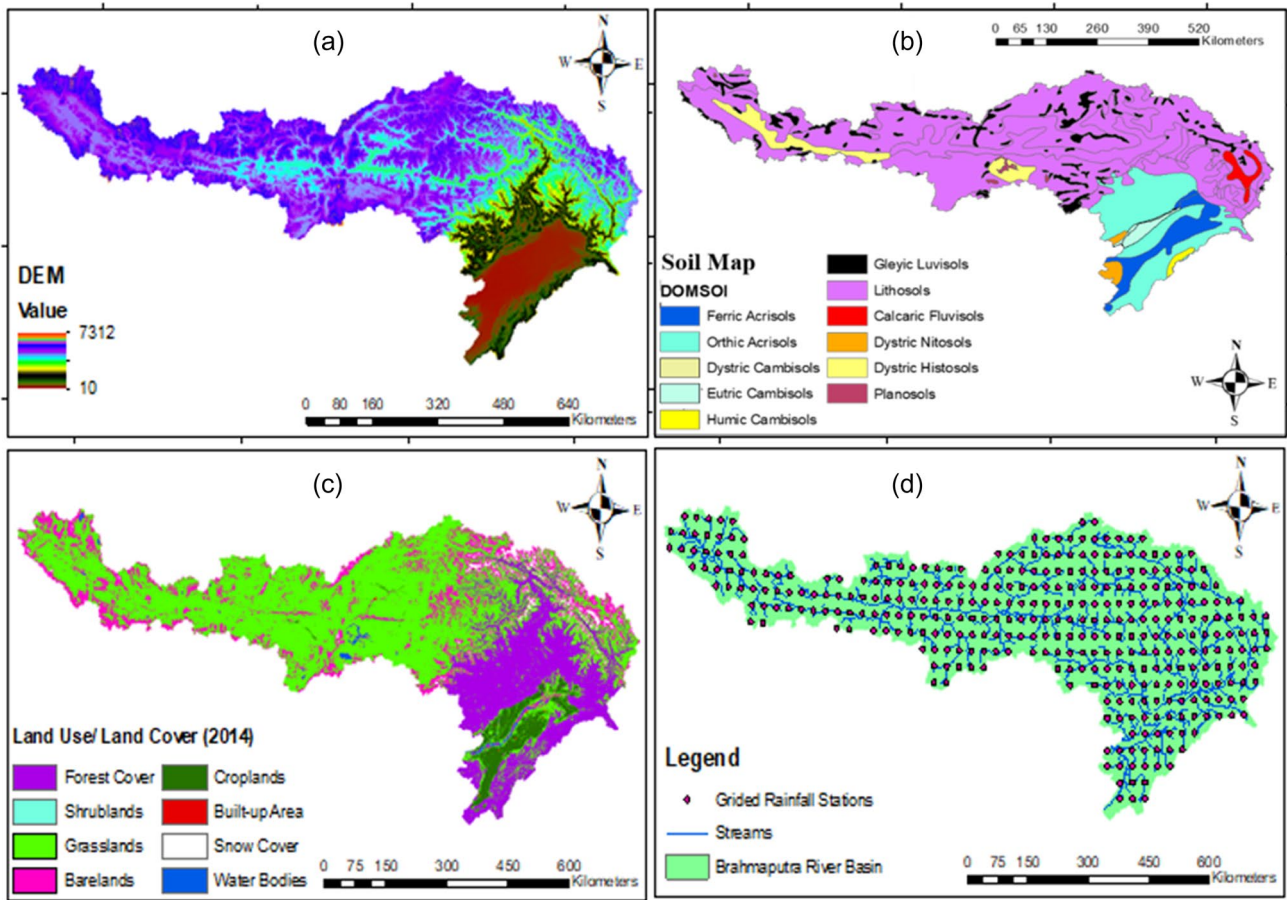


Fig. 2 a DEM map, b soil map, c land use/land cover map for 2014, d GRIDED rainfall station map for the upper Brahmaputra River basin

Table 1 Soil classes for Brahmaputra River basin

Sl. no	Soil class	Area (km ²)	Area (%)
1	Calcaric fluvisols	4619	1.24
2	Dystric nitosols	3132	0.84
3	Dystric cambisols	41	0.000027
4	Eutric cambisols	4146	1.11
5	Ferric acrisols	16,741	4.49
6	Gleyic luvisols	28,048	7.53
7	Lithosols	246,091	66.08
8	Humic cambisols	1489	0.40
9	Orthic acrisols	51,379	13.79
10	Dystric histosols	15,489	4.16
11	Planosols	1210	0.32

Table 2 Land use/land cover classes for Brahmaputra River basin

Sl. no	Categories	2001		2014	
		Area (sq. km)	Area (%)	Area (sq. km)	Area (%)
1	Grasslands	210,435	56.51	213,526	57.34
2	Shrub lands	63	0.017	44	0.012
3	Forest cover	80,956	21.74	80,380	21.59
4	Crop land	15,975	4.29	15,826	4.25
5	Snow	6703	1.8	7075	1.9
6	Built-up area	145	0.039	149	0.040
7	Water bodies	1955	0.525	1825	0.49
8	Bareland	56,081	15.06	53,474	14.36

RUSLE model

The Revised Universal Soil Loss Equation (RUSLE) parameters are generally used # calculate average annual soil erosion in forest and agricultural environments. Wischmeier and Smith (1978) were responsible for introducing and improving the soil erosion factor. Five primary input factors, *R*,

K, *LS*, *C*, and *P*, need the use of the RUSLE model. Each parameter is saved as a raster file, and the annual average soil loss is calculated in Arc GIS using the raster calculator, as shown in Eq. (1).

$$A = R \times K \times LS \times C \times P, \tag{1}$$

where A = Average annual soil erosion rate in t/ha/yr, R = Rainfall erosivity factor in MJ/mm/ha/hr/yr, K = Soil erodibility factor in t/hr/MJ/mm, L = slope length factor in m, and S = Slope steepness factor in (per cent), C = Crop management factor without unit, and P = Conservation practise factor without unit.

Rainfall erosivity factor (R)

Rain's impact on runoff and erosion is encapsulated by the R factor. One of the elements in the RUSLE model is the rainfall erosivity factor, which determines how much rain can erode the soil. This indicates that both the environmental circumstances and the data utilized in rainfall erosivity modeling may have an impact. The quality of available data for the selected research area is currently quite variable. As a result, using (Singh et al. 1981)'s method, the R factor is derived from the interpolated map:

$$R = 79 + 0.363 \times P, \tag{2}$$

where R = Rainfall erosivity factor (MJ/mm/ha/hr/yr), and P = Average annual rainfall (mm).

Soil erodibility factor (K)

Soil erodibility factor (K) specifies how vulnerable different soil types are to erosion and runoff rate (Renard 1997). The K factor indicates the cohesiveness or adhesiveness of soil particles and how prone a particular soil is to erosion on a given slope. The values for specific textural soil classes are derived from the soil erodibility factor (Wischmeier and Smith 1978). The FAO DSMW soil map is used to create the soil texture map for the research area. In the raster calculator class, the K -factor value is estimated using the formula shown below in Eq. (3):

$$K = 0.1317 \times F_{csand} \times F_{cl-si} \times F_{orgC} \times F_{hisand}, \tag{3}$$

where F_{csand} = Factor that lowers the K indicator in soils with high coarse-sand content and raises it in soils with little sand. F_{cl-si} = Factor that yields low soil erodibility factors for soils with high clay-to-silt ratios. F_{orgC} = Factor that lowers K values in soils with high organic carbon content, whereas F_{hisand} = Factor that lowers K values in soils with extremely high sand content. The elements are calculated as follows:

$$F_{csand} = \left[0.2 + 0.3 \cdot \exp \left\{ -0.256 \cdot m_s \left(1 - \frac{m_{silt}}{100} \right) \right\} \right] \tag{3a}$$

$$F_{cl-si} = \left(\frac{m_{silt}}{m_c + m_{silt}} \right)^2 \tag{3b}$$

$$F_{orgC} = \left(1 - \frac{0.25 \cdot orgC}{orgC + \exp[3.72 - 2.95 \cdot orgC]} \right) \tag{3c}$$

$$F_{hisand} = \left(1 - \frac{0.7 \left(1 - \frac{m_s}{100} \right)}{\left(1 - \frac{m_s}{100} \right) + \exp[-5.5 + 22.9 \cdot \left(1 - \frac{m_s}{100} \right)]} \right), \tag{3d}$$

where m_s = sand fraction content of 0.05–2.00 mm diameter (%), m_{silt} = silt fraction content of 0.005–0.05 mm diameter (%), m_c = clay fraction content (<0.002 mm diameter) (%), and $orgC$ = organic carbon (SOC) (%) (Wawer et al. 2005).

Slope length and steepness factor (LS)

The slope steepness directly impacts erosion, as a steeper slope causes more significant erosion. They produce topography on the topsoil erosion, including slope length and steepness that influence surface runoff speed (Risse et al. 1993). Flow accumulation and slope of the study area are required to determine the LS factor. The equation followed by (Bewket and Teferi 2009; Kamaludin et al. 2013) is implemented to find out the LS factor (Eq. 4).

$$LS = (FA \times cell\ size / 22.1)^m \times (0.065 + 0.045S + 0.0065 S^2), \tag{4}$$

where LS = Slope length and Slope steepness factor, FA = Flow accumulation expressed as a no. of grid cells; S = slope gradient in percentage; cell size = Grid cell size or the resolution of a DEM map, and m = exponent that depends upon slope steepness which is listed in Table 3 (Wischmeier and Smith 1978).

Cover and management factor (C)

This factor is defined as the conversion of soil erosion from cultivated land to equal soil erosion from clean tilled and continuous fallow land under particular conditions (Singh and Phadke 2006). The vegetation cover in an area provides resistance to surface flow as well as act as a shield for splash erosion due to rain. Therefore, crop management factor provides an idea about the soil losses that may incurred due to vegetation cover. Because some parts of the basin are

Table 3 Values of exponent m for slope class (Wischmeier and Smith 1978)

Sl. no	Slope class (%)	Value of m
1	Less than 1	0.2
2	1–3	0.3
3	3–5	0.4
4	Greater than 5	0.5

Table 4 Cover management factors (*C*) for each land use/land cover type (Ganasri and Ramesh 2016)

Sl. no	Land use/land cover type	<i>C</i> factor value
1	Water bodies	0
2	Forest	0.003
3	Wasteland	0.5
4	Built-up area	0.09
5	Cropland	0.63
6	Others	0.001

Table 5 Conservation practice factor (*P*) from the land use/land cover classes (Li et al. 2011)

Sl. no	Land use/land cover	<i>P</i> factor values
1	Water bodies	0
2	Built-up areas	0
3	Cropland	0.4
4	Shrublands	1
6	Wetlands	0.7
7	Forest	1
8	Wasteland	1

located in China and Tibet, the *C* factor is unavailable for all crops. As a result, Table 4 shows the *C* values derived in the current study and those are calculated by Ganasri and Ramesh (2016).

Conservation practice factor (*P*)

The influence of land use strategies that limit runoff and thus lower erosion rates for a specific soil type is reflected by the support factor (*P*). The *P* factor depicts the soil loss ratio by a support method to upslope and downslope straight row farming (Wischmeier and Smith 1978). Land use characteristics are considered when considering management measures to reduce soil loss. Because the bulk of the upper Brahmaputra basin lacks suitable management methods, it is preferable to employ Wischmeier and Smith's *P* factor (Wischmeier and Smith 1978). *P* values are used for the current study region, according to Li et al. (2011) (Table 5).

Sediment delivery ratio (SDR)

The RUSLE model only predicts average yearly soil erosion and ignores degraded sediment transit and deposition (Thomas et al. 2018). As a result, the sediment delivery ratio (SDR) can be applied in conjunction with the RUSLE estimate of average soil erosion to calculate the amount of sediments delivered to the watershed area's outlet over a

given time period (Andersson 2010). Williams and Berndt's (1977) equation is used to compute SDR in this study:

$$\text{SDR} = 0.627 \times (\text{SCS})^{0.403}. \quad (5)$$

SCS refers to the slope of the principal river channel in the watershed, which is measured in percentages. ArcGIS is used to compute the slope of the main channel. In the absence of data, the SCS raster grid uses an average upstream cell slope, which has an impact on stream channel sediment delivery capacity.

Sediment yield (SY)

Although RUSLE cannot directly calculate sediment yield, it can be calculated using a combination of RUSLE and SDR (de Rosa et al. 2016). The percentage of eroded soil that does not deposit in the watershed while being transported to the outflow and reaches the downstream area is referred to as sediment yield. Climate, local topography, lithology, basin geometry, drainage networks, and land use/land cover types all have an effect on the sediment yield mechanism in a drainage watershed (Restrepo et al. 2006). Because some areas of the study region lack comprehensive periodic measurements, sediment yield is calculated using SDR and total soil loss. The SDR, which is the ratio of annual specific sediment yield to gross soil erosion (Fistikoglu and Harmancioglu 2002), can be expressed as follows:

$$\text{SY} = \sum_{i=1}^n \text{SDR} \times A. \quad (6)$$

Here, SY = Annual sediment yield (tonne), *A* = yearly soil loss in the *i*th cell of a catchment, as calculated by Eq. (1), and SDR = Sediment delivery ratio. Figure 3 shows the flow-chart of methodology for the RUSLE-SDR model.

SRWA model

The RUSLE and SDR models show that sediment yield is more sensitive to precipitation than other catchment parameters. As shown in Fig. 4, there is an exponent relationship between annual precipitation and sediment yield, with a correlation of 0.52. Moreover, the whole watershed is divided into seven smaller watersheds. Sediment yield is calculated in each watershed using RUSLE and SDR models together. In this watershed, LULC has minimal effect on the change in sediment yield; hence in this model, sediment yield (S_y) is a function of watershed area (*A*) and rainfall (*R*). Based on this variation of sediment, watershed area, and precipitation, one new model is selected here as follows:

Fig. 3 Flow Chart of the methodology of RUSLE and SDR models

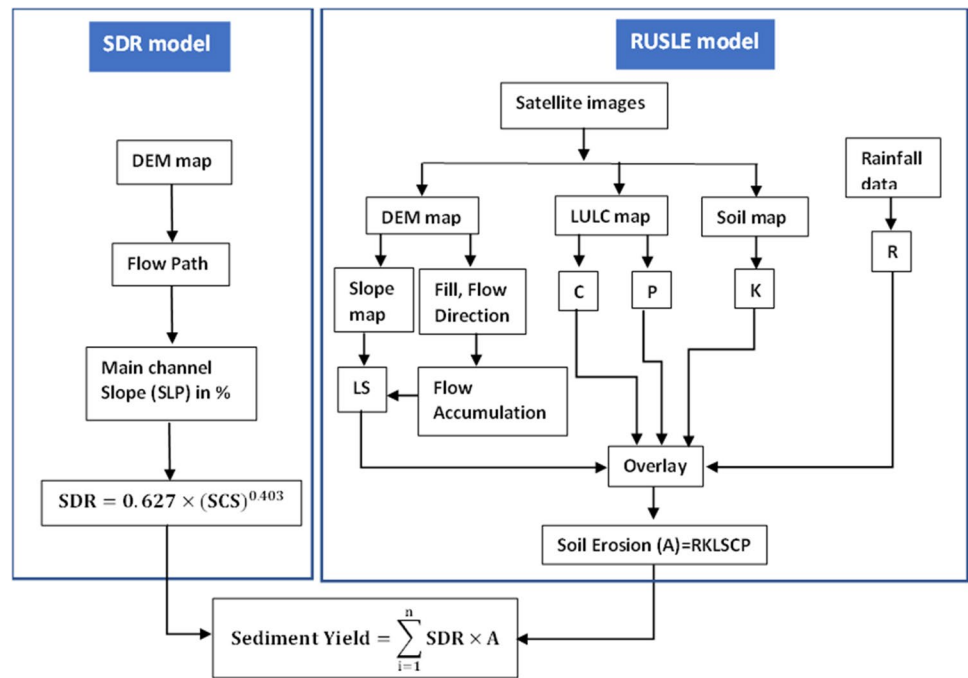
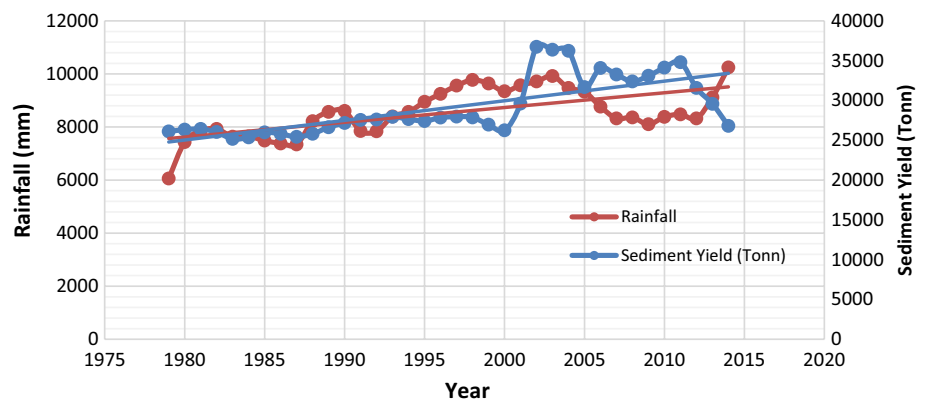


Fig. 4 Relationship between annual rainfall (mm) and sediment yield (tonnes)



$$S_y = f(R, A). \tag{7}$$

It can be written in the form of a nonlinear equation as:

$$S_y^i = \left[\alpha(A^i)^\beta + p(R_y^i)^q \right], \tag{8}$$

where α , β , and p , q is the model parameters constant for A^i and R_y^i , respectively. y denotes the year, and i is the watershed number ranging from 1 to 8; S_y^i = Sediment yield in the i th watershed for y th year (tonne); A^i = Area of i th watershed (sq. km), and R_y^i = rainfall in the i th watershed for y th year (mm).

Generalized reduced gradient (GRG) nonlinear method

In general, a user can use an excel solver to find the best value for an objective function in the target cell of a dataset. The Excel Solver adjusts the user-identified modifiable cells to maximize/minimize another target cell's value by working on the data set directly or indirectly connected to the target cell's goal function. Optimizing sediment model parameters is a highly nonlinear problem (Luo and Xie 2010). This tool can calibrate the design parameters of the sediment yield model developed in this study using powerful search techniques. The generalized reduced gradient (GRG) solver is used in this approach (Lasdon et al. 1978; Murtagh and Saunders 1978; Smith and Lasdon 1992). Leon Lasdon developed the GRG solver, a nonlinear optimization tool. GRG and its implementation have been demonstrated

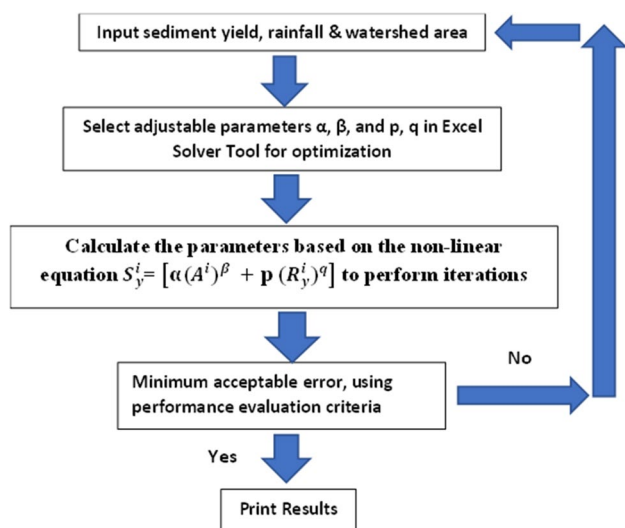


Fig. 5 Flow Chart of the methodology of SRWA model

to be one of the most resilient and dependable techniques for solving challenging nonlinear programming problems over a longer period (Smith and Lasdon 1992). The optimization of these models was done with Microsoft Excel's solver extension and was based on Roddy's initial configuration (Roddy 2010). The generalized reduced gradient (GRG) nonlinear technique is utilized to estimate model parameters in this investigation. The GRG model creates solutions with ranks considering the variables with cross-over and mutation probability. The parameter sets are chosen that satisfy the objective function with the best solution. The GRG-nonlinear approach uses the multi-start parameter to boost the likelihood of a globally optimal solution. Figure 5 shows the flowchart of methodology for the SRWA model. The GRG nonlinear algorithm calculates the four coefficients in Eq. (8) using the Excel solver tool in this model. Model data are imported for the three variables rainfall, sediment yield, and watershed area based on the RUSLE-SDR model. In the SRWA model, the values for the four coefficients α , β , and p , q are estimated using optimization technique in excel solver.

Performance evaluation criteria

Several performance evaluation criteria are established to compare the results of different approaches (Mohan 1997; Toprak et al. 2009; Luo and Xie 2010). The following assessment criteria validate the Excel solver's and other parameter estimate algorithms' efficacy. The following indices were used to evaluate the performance of various parameter estimate approaches in terms of the relationship between observed and expected discharges. Standard statistical criteria such as the "coefficient of correlation" (CC), Nash–Sutcliffe model "efficiency coefficient" (CE) (Nash and Sutcliffe 1970), and root-mean-square error

(RMSE) are used to assess the performance of the model. The direction and intensity of a linear relationship between observed and simulated data are measured by the correlation coefficient (CC) (Heathman et al. 2009). Negative and positive linear correlations are represented by plus and minus signs, with values ranging from -1.0 to +1.0. The "efficiency coefficient" (CE) is an essential statistic for accounting the model fitness. The CE goes from 0.0 to 1.0, with 1.0 being the best. Values between 0 and 1 are considered acceptable; however, values less than 0 are not acceptable and indicate poor performance between the observed and simulated data (Jabbar and Yadav 2022). The RMSE is the residuals' standard deviation (prediction errors). It ranges from an optimal 0.0 to a big positive number and is determined as the ratio of RMSE to the standard deviation of the observed data.

Correlation coefficient (CC)

$$= \frac{N(\sum(Q_o Q_p) - (\sum Q_o)(\sum Q_p))}{\sqrt{(N(\sum(Q_o^2) - (\sum Q_o)^2)(N(\sum(Q_p^2) - (\sum Q_p)^2))}} \quad (9)$$

$$\text{Nash – Sutcliffe Efficiency (CE)} = 1 - \frac{\sum_{i=1}^N (Q_o^i - Q_p^i)^2}{\sum_{i=1}^N (Q_o^i - \bar{Q}_o)^2} \quad (10)$$

$$\text{Root mean square Error (RMSE)} = \sqrt{\frac{\sum_{i=1}^n (Q_o^i - Q_p^i)^2}{N}} \quad (11)$$

where i = variable ranges from 1 to n , n = total number of data, N = number of non-missing data points, Q_o is sediment yield of SRWA model; Q_p is simulated sediment yield of RUSLE-SDR model, and \bar{Q}_o = mean sediment yield of SRWA model.

Results and discussion

RUSLE-based soil loss estimation

A sediment yield model (SRWA model) is developed using the estimated value obtained from the RUSLE-SDR model. The model is developed using simple numerical techniques with the help of an excel solver, although the data used in the excel solver are generated with the help of spatial techniques like Arc GIS. To calculate the sediment output at the watershed outlet, the rainfall erosivity factor (R) is calculated using daily precipitation data (mm) from 357 gauging sites from 2001 to 2014. (Fig. 2e). The total amount of rainfall divided by the total number of rainy days yields the average annual rainfall. While observing

the rainfall data for the entire Brahmaputra River basin, it is found that the rainfall distribution is highly heterogeneous. In most of the area, the downstream portion of the river receives comparatively higher precipitation, whereas the extreme upstream portion receives only snowfall. The downstream region near Majuli River Island receives the maximum rainfall, 2216 mm per year. To calculate spatial interpolation of rainfall data, ArcGIS uses the inverse distance weightage (IDW) method. With the help of Eq. (2), the R factor map is prepared for every year starting from 2001 to 2014. It can be observed from Fig. 6a that rainfall erosivity is high near the downstream sections of Majuli, whereas lower values are found in the middle and upstream portions of the watershed. After preparing the rainfall erosivity factor map, with the help of the soil texture map and using Eq. (3), the soil erodibility factor (K) map is prepared. From Table 1, it is found that lithosols and Acrisols are the dominant soil types found in the watershed. About 66.09% and 13.80% of the total study area are occupied by lithosols and Acrisols soil classes. Lithosols soil mostly consists of stones and rocks at the surface level. In the lithosols soils, the soil texture is more porous, leading to low water holding capacity (Triharyanto 2018). Acrisols soil type possesses low inherent fertility and is subjected to erosion on exposed slopes (Dent 1980). From the calculation done using Eq. (3), the values of the K factor vary from 0.0167 to 0.0233 and are shown in Fig. 6b. From the spatial distribution map, it has been observed that the soil erodibility factor (K) is found to vary from high to low from the upper Brahmaputra watershed to lower elevated areas, respectively. The values of K are found to be significantly high in the highest elevated part which indicates that the soil is more prone to erosion subject to receive of sufficient rainfall. The soil of the lower Brahmaputra basin is combined with clay particles, which provide higher erosion resistance.

Another important parameter to estimate soil erosion from a basin is its slope length and the steep factor (LS). The higher the slope of a basin, the lower the resistance during the surface flow, increasing more erosion towards the end. Therefore, the (LS) factor calculation becomes significant when estimating surface erosion. LS factor is calculated using Eq. (4) with the help of a slope and flow accumulation map extracted from DEM in the GIS platform. In this study, the highest elevation areas are found near the Tibet region of the Himalayan Mountain range, and the lower part of the basin resides in Arunachal and Assam, in India. While calculating the slope factor, the DEM is preprocessed in ArcGIS by filling the sinks and other depression areas; otherwise, it will provide some errors at the end of the programme. The exponent ' m ' mentioned in Eq. (4) varies with the slope in a basin, and its values can be found in Table 3. Finally, the LS value for the selected study area is calculated and mapped in Fig. 6c, where it can

be observed that the value ranges from 0 to 51.74. The LS factor map shows that the lower LS values are found in plain areas near Majuli, where the land is mainly used for farming and settlement.

The LULC maps of 2001–14 (Fig. 2c) are used to prepare crop management factor (C) maps. From Table 2, it is observed that in 2014, grasslands (57.34%) and forest cover (21.59%) are the two LULC classes that cover maximum watershed areas. It can also be seen that the change in LULC from 2001 to 2014 is minimal (Table 2). The crop management factor (C) maps for 2001–14 are created by reclassifying each land use category using the C values from Table 4. The C factor is determined to be between 0 and 0.63. (Fig. 6d). In 2014, it was discovered that grasslands and forests cover 57.34% and 21.59% of the watershed area, respectively (Table 2). For forest and farmland, C factor values of 0.5 and 0.003 are found in the majority of basin areas, respectively. Table 5 shows how the P factor maps for the years 2001–14 are created using the spatial analysis software in GIS. Due to a lack of data on conservation activities in some areas, the P factor value across the bulk of the watershed that is covered by forest is assumed to be 1. The watershed's P factor values are observed to range from 0 to 1. (Fig. 5e). The watershed's centre section has seen the most considerable conservation values, followed by the northeast.

The average annual soil loss maps for 2001–2014 are generated using the five RUSLE factors as R , K , LS , C , and P factors (Fig. 6f). The map is prepared by multiplying map layers of all the factors on a 30×30 m resolution grid using GIS by a cell-by-cell analysis. The current study's findings show a complex change in soil erosion caused by variations in rainfall amount over the study period. The watershed's average annual rainfall has increased in the north-eastern and downstream regions. This variation in rainfall amount has resulted in a shift in the pattern of soil loss rate over this time period. Critical soil loss levels are found in the north-eastern portions of the basin, where the most significant amount of soil loss is identified. After analysing the data and thematic maps, it is found that the study area produces a high rate of soil erosion amount. However, the higher elevated area produces less erosion, the central and downstream portions of the watershed yield high sediment.

Sediment yield estimation

The watershed's DEM is utilized to construct the flow route, which is then used by ArcGIS Tools to calculate the average mainstream channel slope for each raster grid. Equation (5) is used to create a sediment delivery ratio map. The SDR values for the major river channel in the basin range from 0 to 1. (Fig. 6g). Because the northeast section has steeper topography, the SDR values in the upstream and northeast

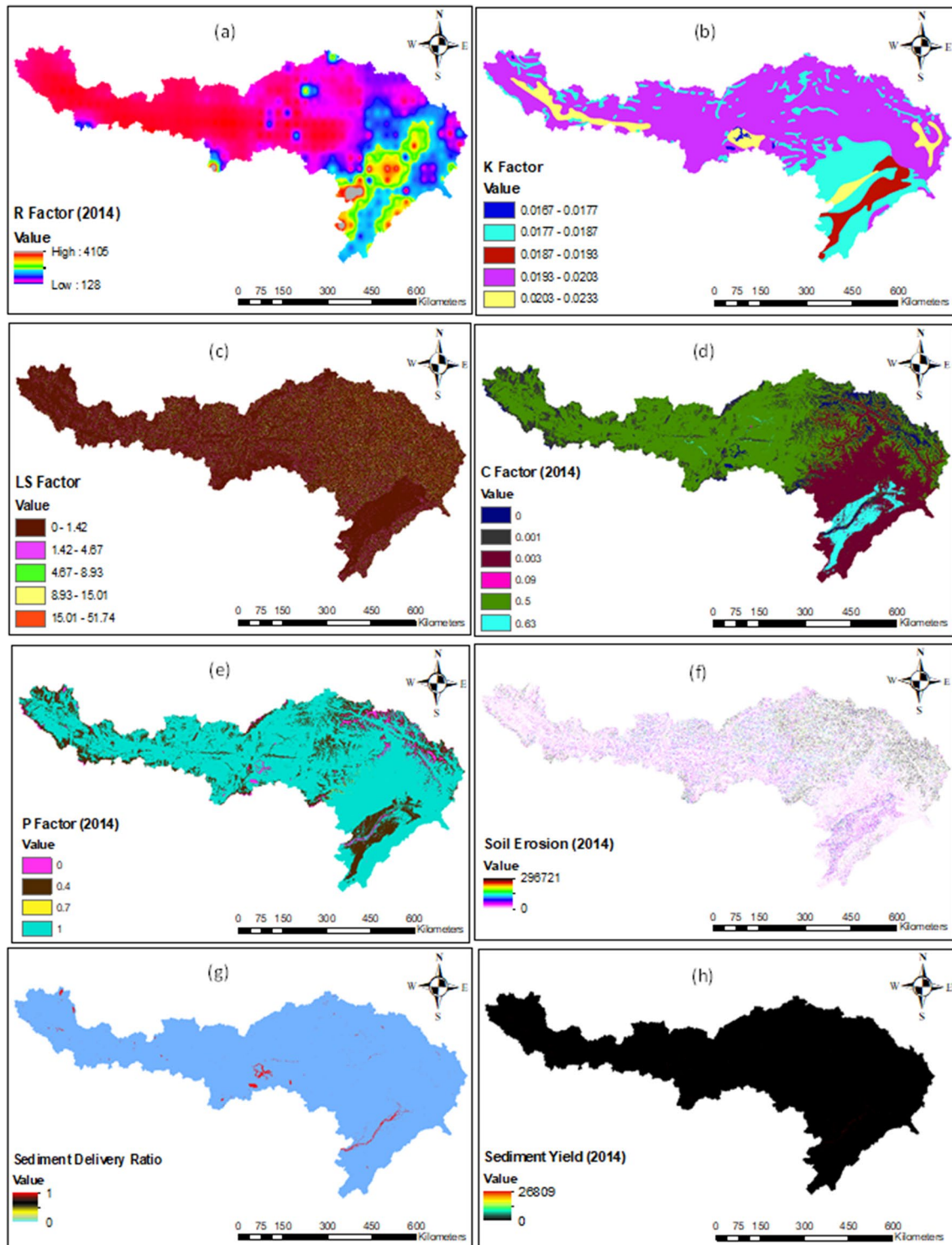


Fig. 6 **a** Rainfall erosivity factor (R) map for 2014, **b** soil erodibility factor (K) map, **c** slope length and steepness factor (LS) map, **d** cover and management factor for 2014, **e** conservation practice

factor (P) maps for 2014, **f** average annual soil erosion rate map for 2014, **g** slope-based SDR map at flow path draped over DEM, **h** annual sediment yield map for the year 2014

regions of the watershed are greater. As a result, more eroded material will be moved into the channels and delivered to the outlet of the catchment from upstream places.

Annual sediment yield maps for 2001–2014 are calculated by superimposing the SDR map over the annual soil erosion map using Eq. (6). As a result, the sediment output predicted

Table 6 Sediment yield (tonne) at different watershed outlets estimated by SDR-RUSLE model

Watershed	Calibration period		Validation period	
	Year	Sediment yield (tonne)	Year	Sediment yield(tonne)
1	2001	30,504	2008	32,386
	2002	36,739	2009	33,100
	2003	36,368	2010	34,122
	2004	36,237	2011	34,813
	2005	35,989	2012	31,569
	2006	34,083	2013	29,569
	2007	33,257	2014	26,809
2	2001	29,604.1	2008	22,822.5
	2002	30,427	2009	27,413.8
	2003	31,182.6	2010	28,260.4
	2004	28,609	2011	28,832.6
	2005	31,675	2012	26,145.8
	2006	28,227	2013	29,569.2
	2007	27,544	2014	26,809
3	2001	21,008	2008	21,034.8
	2002	21,044	2009	20,378.3
	2003	21,329	2010	21,785.2
	2004	21,233	2011	22,304.6
	2005	21,569	2012	21,834.6
	2006	21,214	2013	21,544.6
	2007	21,223	2014	21,387
4	2001	18,513.7	2008	16,538
	2002	13,099	2009	16,469
	2003	13,389	2010	16,693
	2004	14,859	2011	16,278
	2005	16,385	2012	16,444
	2006	16,978	2013	15,910
	2007	15,634.8	2014	15,823
5	2001	7512	2008	6870
	2002	7660	2009	8251
	2003	8068	2010	8691
	2004	7964	2011	9204
	2005	8245	2012	9142
	2006	8174	2013	9439
	2007	8356	2014	8219
6	2001	4020	2008	4399
	2002	4450	2009	4632
	2003	4275	2010	4898
	2004	4504	2011	4922
	2005	4467	2012	5145
	2006	4317	2013	5043
	2007	4445	2014	4930

Table 6 (continued)

Watershed	Calibration period		Validation period	
	Year	Sediment yield (tonne)	Year	Sediment yield(tonne)
7	2001	1935	2008	1896
	2002	2028	2009	1924
	2003	1932	2010	1971
	2004	2053	2011	1988
	2005	2038	2012	1987
	2006	1988	2013	1975
	2007	1900	2014	1470
8	2001	1528	2008	1388
	2002	1510	2009	1410
	2003	1524	2010	1414
	2004	1514	2011	1438
	2005	1498	2012	1466
	2006	1456	2013	1470
	2007	1420	2014	1381

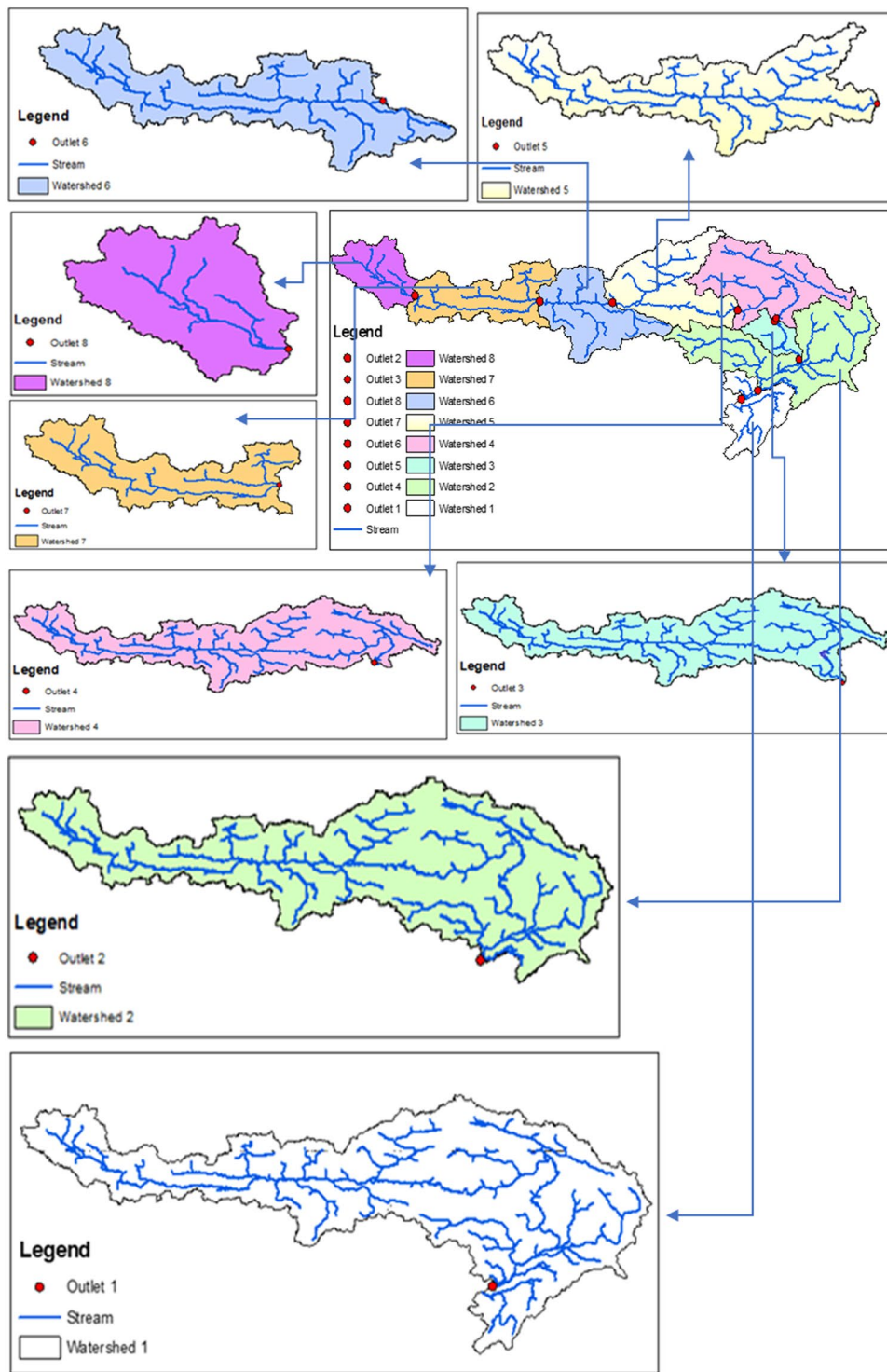
along the whole basin's mainline up to Majuli River Island in 2014 ranges from 0 to 26,809 tonnes (Fig. 6h).

SRWA model parameters estimation

The RUSLE model-based sediment yield has seen changes in rainfall variability that have influenced sediment output during these periods (Table 6). In this case, the sediment-rainfall model parameters α , β , and p , q , should be computed for four parameters to calibrate the model for the selected watershed. A single objective function developed using Eq. (8) determines the sediment-rainfall series parameters to calibrate the models to meet the continuity requirement. An efficient optimization routine is necessary to estimate parameters with an objective function. Hence, the "Excel solver," which is simple to use, is used to find the model parameters. Parameter set values for the model are estimated for two cases: first calibration period (2001–2007) and then verification period (2008–2014), considering rainfall as the only variable. As sediment yield is a function of watershed area and rainfall in that watershed, sediment yield at the outlet of a watershed can be associated with the watershed area and total rainfall in a particular year. This relationship is shown using Eq. (8).

The whole watershed is divided into seven more sub-watersheds taking outlets at seven different locations within the watershed. Sediment yield is calculated at each of the watershed (Fig. 7). Parameter values for Eq. (8) are estimated using the Excel solver's optimization technique (GRG

Fig. 7 Maps showing all the eight watersheds



nonlinear method). The parameter values are discovered to be $= 1.39045, = -5.92783, p = 1.26481,$ and $q = 1.10855$ after a few optimization trials. In Fig. 8, a graphical display of sediment yield calculated by the SRWA and SDR-RUSLE models is plotted for the calibration period (2001–2007). Figure 9 shows the comparison between sediment yields (tonne) of SRWA model and sediment yield (tonne)

RUSLE-SDR model for verification period (2008–2014). Table 7 shows the model's statistical results during the calibration and verification periods. The statistical results reveal that the correlation coefficient (CE) for the calibration and verification periods is 0.969 and 0.964, respectively. The Nash–Sutcliffe coefficient of efficiency for the same period is 0.89 and 0.87, which is regarded as excellent. Table 7 shows

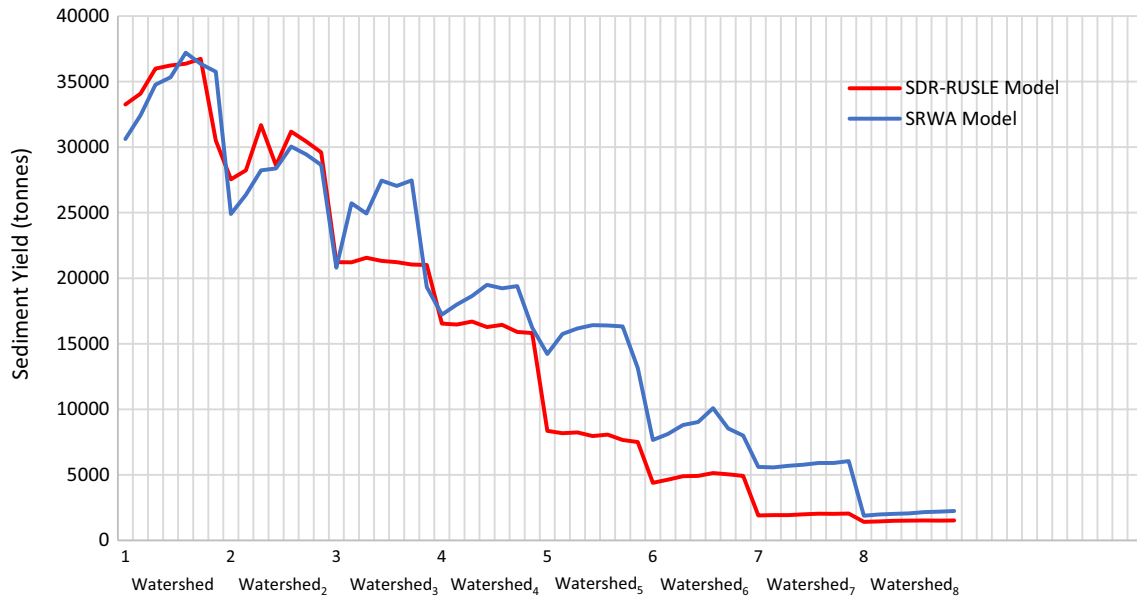


Fig. 8 Comparison between sediment yields (tonne) of SRWA model and sediment yield (tonne) RUSLE-SDR model for 2001–07 for the upper Brahmaputra River basin

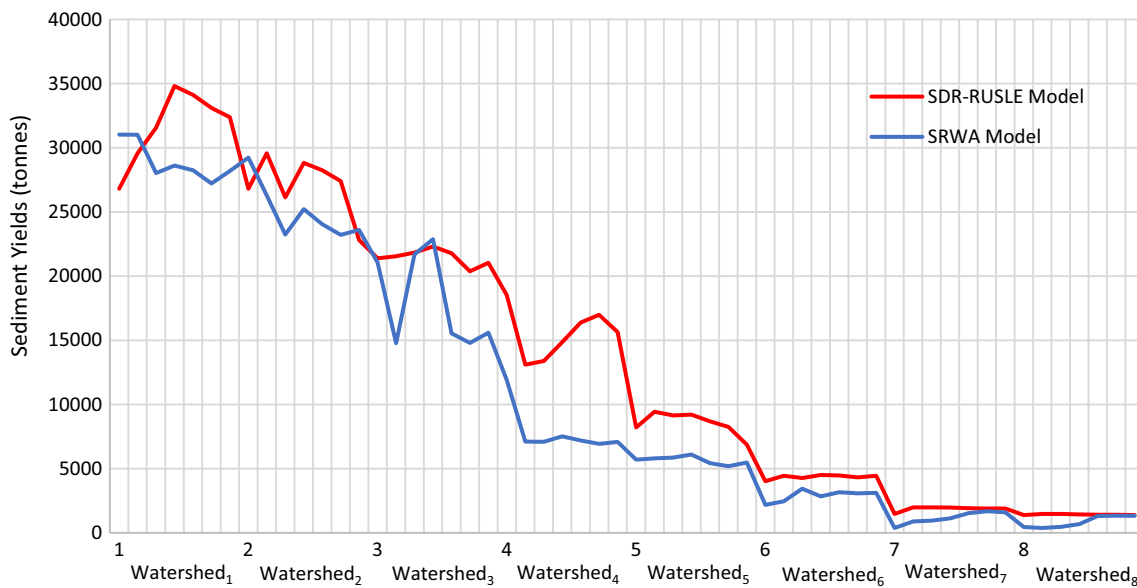


Fig. 9 Comparison between sediment yields (tonne) of SRWA model and sediment yield (tonne) RUSLE-SDR model for 2008–14 for the upper Brahmaputra River basin

Table 7 Model performance in comparison with sediment yield using the RUSLE model in the Brahmaputra River basin

Sl. No	Performance index	Calibration period (2001–07)	Validation period (2008–14)	Overall performance (2001–2014)
1	Efficiency coefficient (CE)	0.89	0.87	0.88
2	Coefficient of correlation (CC)	0.97	0.96	0.96
3	Root mean square error (RMSE)	3914	3810	3957

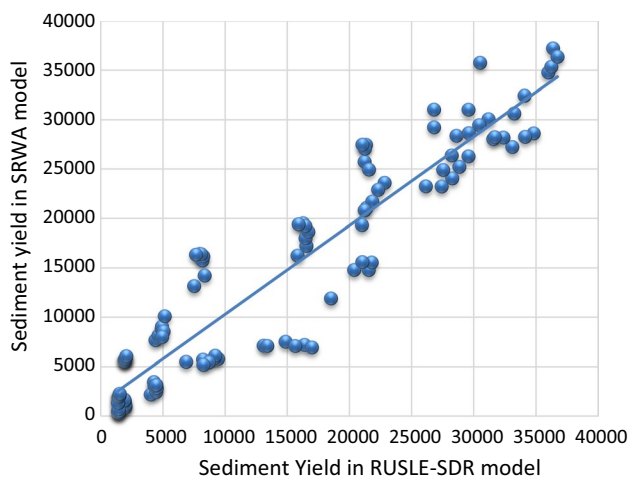


Fig. 10 Scatter plot between sediment yields (tonne) of SRWA model and sediment yield (tonne) RUSLE-SDR model for 2001–14

the statistical performance in detail, revealing a strong correlation between the recently developed SRWA model and the SDR-RUSLE model. The estimated sediment graph for the calibration and verification periods is shown in Figs. 8 and 9. Figure 10 depicts the scatter plot of data obtained by the SRWA and SDR-RUSLE models for calibration and verification periods (2001–2014).

In this study, the newly developed SRWA model has shown satisfactory performance during the calibration and validation processes. It can be seen that the GRG solver has found the optimal solution in about 100 iterations. Based on the above results, it can be observed that the GRG solver has shown comparatively good results in terms of CE, CC, and RMSE. Also, the GRG solver finds optimal solution for all the four sediment yield parameters. The implementation of the SRWA model at a sub-watershed level is simpler than other methods for sediment yield estimation. Therefore, the output of this model has excellent results with reasonable accuracy. Thus, in a larger watershed like the Brahmaputra River Basin, SRWA model can be applied to estimate sediment yield taking outlet at different locations of the watershed.

Conclusions

The upper Brahmaputra River basin's soil erosion and sediment output are examined utilizing an integrated RUSLE-SDR model in a GIS platform. All the thematic maps like *R* factor, *K* factor, *LS* factor, *C* factor, and *P* factor which are required to estimate soil erosion and sediment yield have been prepared. The developed map shows that the

higher elevated areas have good vegetation cover with better support practice, which reduces soil erosion. On the other hand, the lower elevated portion produces more erosion and significant sediment yields. The present study applies the RUSLE and SDR models for eight watersheds in the upper Brahmaputra River basin to Majuli River Island. The sediment yield data are created from 2001 to 2014 using the SDR-RUSLE model. The information is further divided into two periods: calibration (2001–2007) and verification (2008–2014). A new model called the SRWA model has been constructed and calibrated for 2001–2008 and verified for 2008–2014. The SRWA model is calibrated in this study using a basic optimization approach (GRG nonlinear) available in the Excel solver. Thus, the Nash–Sutcliffe coefficient of efficiency of the model for calibration and verification period is 0.89 and 0.87, respectively. Hence, the new model can estimate sediment yield at any watershed/sub-watershed using input data such as watershed area and annual rainfall by calibrating the new model with sediment yield data obtained by the SDR-RUSLE model. Although the model performs well statistically in this investigation, there is still room for improvement using a better optimization strategy. In this sediment model, SRWA estimates the sediment yield occurrence at the sub-watershed level by only considering the most effective factors. But there may be other existing and actual sediment features, which may influence sediment yield amount somewhat from the actual values. Moreover, there may be data inefficiencies and model errors. This variation may cause some uncertainties in the result of the model. Also, we have limited this work within the above three influential parameters only by taking negligible effect of other parameters, although the model may not work in other additional parameters. Besides, this SRWA model is tested in a single watershed only and may not be suitable for different types of watersheds with different climatic and watershed characteristics. Further, this model should be applied to other kinds of the watershed by taking some additional influential parameters. In many watersheds, soil and riverbank erosion are common occurrences requiring attention. The method provided here can assess a watershed's sediment yield pattern and can be extended as needed. The study mentioned in this paper can be applied to another river basin to develop a numerical model to ease the estimation of soil erosion and sediment yield, which requires policymakers to make proper management decisions.

Declarations

Conflict of interest The authors confirm there is no conflict of interest in the manuscript.

References

- Alewell C, Borrelli P, Meusburger K, Panagos P (2019) Using the USLE: chances, challenges and limitations of soil erosion modelling. *Int Soil Water Conserv Res* 7(3):203–225
- Andersson L (2010) Soil loss estimation based on the USLE/GIS approach through small catchments—a minor field study in Tunisia. *TVVR*10/5019
- Bewket W, Teferi E (2009) Assessment of soil erosion hazard and 412 prioritization for treatment at the watershed level: case study in the Chemoga watershed, Blue Nile basin. *Ethiop Land Degrad Dev* 20(6):609–622
- Bhattacharyya R, Ghosh BN, Mishra PK, Mandal B, Rao CS, SarkarDasLalithaHatiFranzluibbers DKMKAJ (2015) Soil degradation in India: challenges and potential solutions. *Sustainability* 7(4):3528–3570
- De Rosa P, Cencetti C, Fredduzzi A (2016) A GRASS tool for the Sediment Delivery Ratio mapping. *PeerJ Preprints* 4:e2227v1
- Dent FJ (1980) Major production systems and soil-related constraints in Southeast Asia. In: *Priorities for alleviating soil-related constraints to food production in the tropics*, pp 79–106
- Duru U, Arabi M, Wohl EE (2018) Modeling stream flow and sediment yield using the SWAT model: a case study of Ankara River basin. *Turk Phys Geogr* 39(3):264–289
- Fistikoglu O, Harmancioglu NB (2002) Integration of GIS with USLE in assessment of soil erosion. *Water Resour Manage* 16(6):447–467
- Ganasri BP, Ramesh H (2016) Assessment of soil erosion by RUSLE model using remote sensing and GIS—A case study of Nethravathi basin. *Geosci Front* 7(6):953–961
- Gelagay HS (2016) RUSLE and SDR model based sediment yield assessment in a GIS and remote sensing environment; a case study of Koga watershed, Upper Blue Nile basin. *Ethiop Hydrol Curr Res* 7(2):239
- Girmay G, Moges A, Muluneh A (2020) Estimation of soil loss rate using the USLE model for Agewmaryiam Watershed, northern Ethiopia. *Agric Food Secur* 9(1):1–12
- Hazarika N, Das AK, Borah SB (2015) Assessing land-use changes driven by river dynamics in chronically flood affected Upper Brahmaputra plains, India, using RS-GIS techniques. *Egypt J Remote Sens Space Sci* 18(1):107–118
- Heathman GC, Larose MYRIAM, Ascough JC (2009) Soil and water assessment tool evaluation of soil and land use geographic information system data sets on simulated stream flow. *J Soil Water Conserv* 64(1):17–32
- Hosseini FS, Choubin B, Mosavi A, Nabipour N, Shamshirband S, Darabi H, Haghghi AT (2020) Flash flood hazard assessment using ensembles and Bayesian-based machine learning models: application of the simulated annealing feature selection method. *Sci Total Environ* 711:135–161
- Hurni H, Meyer K (2002) *A world soils agenda: discussing international actions for the sustainable use of soils*. Geographica Bernensia, Bern
- Immerzeel W (2008) Historical trends and future predictions of climate 446 variability in the Brahmaputra basin. *Int J Climatol J R Meteorol Soc* 28(2):243–254
- Issaka S, Ashraf MA (2017) Impact of soil erosion and degradation on water quality: a review. *Geol Ecol Landsc* 1(1):1–11
- Jabbar YC, Yadav SM (2022) Development of reservoir capacity loss model using bootstrapping of sediment rating curves. *ISH J Hydraul Eng* 28(sup1):14–26
- Jain MK, Kothiyari UC (2000) Estimation of soil erosion and sediment yield using GIS. *Hydrol Sci J* 45(5):771–786
- Kamaludin H, Lihan T, Ali Rahman Z, Mustapha MA, Idris WMR, Rahim SA (2013) Integration of remote sensing, RUSLE and GIS to model potential soil loss and sediment yield (SY). *Hydrol Earth Syst Sci Discuss* 10(4):4567–4596
- Lasdon LS, Waren AD, Jain A, Ratner M (1978) Design and testing of a generalized reduced gradient code for nonlinear programming. *ACM Trans Math Softw (TOMS)* 4(1):34–50
- Li X, Wu B, Wang H, Zhang J (2011) Regional soil erosion risk assessment in Hai Basin. *Yaogan Xuebao J Remote Sens* 15(2):372–387
- Li P, Zang Y, Ma D, Yao W, Holden J, Irvine B, Zhao G (2020) Soil erosion rates assessed by RUSLE and PESERA for a Chinese Loess Plateau catchment under land-cover changes. *Earth Surf Proc Land* 45(3):707–722
- Luo J, Xie J (2010) Parameter estimation for nonlinear Muskingum model based on immune clonal selection algorithm. *J Hydrol Eng* 15(10):844–851
- Mani P, Kumar R, Chatterjee C (2003) Erosion study of a part of Majuli River-Island using remote sensing data. *J Indian Soc Remote Sens* 31(1):12–18
- Mirzaei G, Soltani A, Soltani M, Darabi M (2018) An integrated data-mining and multi-criteria decision-making approach for hazard-based object ranking with a focus on landslides and floods. *Environ Earth Sci* 77(16):1–23
- Mohan S (1997) Parameter estimation of nonlinear Muskingum models using genetic algorithm. *J Hydraul Eng* 123(2):137–142
- Murtagh BA, Saunders MA (1978) Large-scale linearly constrained optimization. *Math Program* 14(1):41–72
- Nash JE, Sutcliffe JV (1970) River flow forecasting through conceptual models part I—A discussion of principles. *J Hydrol* 10:282–290
- Niazkar M, Zakwan M (2021) Assessment of artificial intelligence models for developing single-value and loop rating curves. *Complexity* 2021:1–21
- Poirier C, Poitevin C, Chaumillon E (2016) Comparison of estuarine 479 sediment record with modelled rates of sediment supply from a western European catchment since 1500. *CR Geosci* 348(7):479–488
- Pradeep GS, Krishnan MV, Vijith H (2015) Identification of critical soil erosion prone areas and annual average soil loss in an upland agricultural watershed of Western Ghats, using analytical hierarchy process (AHP) and RUSLE techniques. *Arab J Geosci* 8(6):3697–3711
- Renard KG (1997) *Predicting soil erosion by water: a guide to conservation planning with the Revised Universal Soil Loss Equation (RUSLE)*. United States Government Printing, Washington
- Restrepo JD, Kjerfve B, Hermelin M, Restrepo JC (2006) Factors controlling sediment yield in a major South American drainage basin: the Magdalena River, Colombia. *J Hydrol* 316(1–4904):213–232
- Risse LM, Nearing MA, Laffen JM, Nicks AD (1993) Error assessment in the universal soil loss equation. *Soil Sci Soc Am J* 57(3):825–833
- Roddy BP (2010) The use of the sediment fingerprinting technique to quantify the different sediment sources entering the Whangapoua Estuary, North Island, in New Zealand (Doctoral dissertation, University of Waikato)
- Saha SK (2003) Water and wind induced soil erosion assessment and monitoring using remote sensing and GIS. *Satellite remote sensing and GIS applications in agricultural meteorology*. Jul 7:315–330
- Singh G, Babu R, Chandra S (1981) Soil loss and prediction research in India. In: *Central Soil and Water Conservation Research Training Institute Bulletin*, vol 9, T–12
- Singh R, Phadke VS (2006) Assessing soil loss by water erosion in Jamni River basin, Bundelkhand region, India, adopting universal soil loss equation using GIS. *Current Sci* 90:1431–1435
- Smith S, Lasdon L (1992) Solving large sparse nonlinear programs using GRG. *ORSA J Comput* 4(1):2–15

- Thomas J, Joseph S, Thrivikramji KP (2018) Assessment of soil erosion in a tropical mountain river basin of the southern Western Ghats, India using RUSLE and GIS. *Geosci Front* 9(3):893–906
- Toprak ZF, Eris E, Agiralioğlu N, Cigizoglu HK, Yilmaz L, Aksoy-CoskunAndicAlganci HHGGU (2009) Modeling monthly mean flow in a poorly gauged basin by fuzzy logic. *Clean: Soil, Air, Water* 37(7):555–564
- Triharyanto E (2018) The application of biofilm biofertilizer-based organic fertilizer to increase available soil nutrients and spinach yield on dry land (a study case in lithosol soil type). In: IOP conference series: earth and environmental science, vol 200, no. 1. IOP Publishing, p 01200
- Vale SS, Fuller IC, Procter JN, Basher LR, Smith IE (2016) Characterization 513 and quantification of suspended sediment sources to the Manawatu River, New Zealand. *Sci Total Environ* 543:171–186
- Wawer R, Nowocien E, Podolski B (2005) Eal and calculated kusle erobility factor for selected Polish soils. *Pol J Environ Stud* 14(5):655–658
- Wenzel HG Jr, Melching CS (1987) An Evaluation of the MULTISED (multiple watershed storm water and sediment runoff simulation) simulation model to predict sediment yield. Construction Engineering Research Lab (ARMY), Champaign
- Williams JR, Berndt HD (1977) Sediment yield prediction based on watershed hydrology. *Transactions of the ASAE* 20(6):1100–1104
- Wischmeier WH, Smith DD (1978) Predicting rainfall erosion losses: a guide to conservation planning (No. 537). In: Department of Agriculture, Science and Education Administration
- Xu K, Peng HQ, Rifu DGJ, Zhang RX, Xiao H, & Shi Q (2015) Sediment yield simulation using SWAT model for water environmental protection in an agricultural watershed. *Applied Mechanics and Materials*, vol 713. Trans Tech Publications Ltd, pp 1894–1898
- Yadav A, Joshi D, Kumar V, Mohapatra H, Iwendi C, Gadekallu TR (2022) Capability and robustness of novel hybridized artificial intelligence technique for sediment yield modeling in Godavari River. *India Water* 14(12):1917
- Yan R, Zhang X, Yan S, Chen H (2018) Estimating soil erosion response to land use/cover change in a catchment of the Loess Plateau, China. *Int Soil Water Conserv Res* 6(1):13–22
- Zakwan M, Ahmad Z (2021) Analysis of sediment and discharge ratings of Ganga River. *India Arab J Geosci* 14(19):1–15

Springer Nature or its licensor (e.g. a society or other partner) holds exclusive rights to this article under a publishing agreement with the author(s) or other rightsholder(s); author self-archiving of the accepted manuscript version of this article is solely governed by the terms of such publishing agreement and applicable law.